THE BELL SYSTEM TECHNICAL JOURNAL
Vol. 59, No. 2, February 1980
*Printed in U.S.A.*

# Efficient Calculation of Current Flow in Electroplating Cells

By JAMES L. BLUE

(Manuscript received August 31, 1979)

*An efficient computational method has been developed for calculating the current density distribution within electroplating cells. The computer program can analyze two-dimensional cells with arbitrary polygonal shapes, as well as three-dimensional axisymmetric cells with arbitrary polygonal cross section. Laplace's equation in the bulk of the cell is coupled to the convective diffusion equation in the boundary layers near the electrodes. Finite-difference and finite-element methods, and infinite sums, are avoided by a boundary integral formulation for the solution of Laplace's equation. The method is illustrated with sample calculations for copper plating of multilayer boards. The predicted copper plating thickness distribution is essentially the same as the primary current distribution.*

## I. INTRODUCTION

Until recently, analytic and numerical techniques have not been available for analyzing electroplating cells. Even after the work of Newman and coworkers,[1] only restricted geometries were practical. Design of new electroplating systems has therefore necessarily been done by educated guess, rule of thumb, extrapolation from previous systems, and expensive experimentation. Although the physical and chemical processes taking place in a real-life electroplating cell are generously complex and nonlinear, realistic mathematical models can be constructed, and it is within the state of the computing art to solve these models efficiently.

This paper describes a computer program to solve the mathematical models describing a wide variety of electroplating cells. An important consideration during this development has been that the resulting computer program be able to analyze many different cell geometries and flow patterns with at most trivial program changes. A second consideration has been that the program be efficient and inexpensive

to run, since many geometry and parameter studies are likely to be made in the design or analysis of an electroplating system.

The method is illustrated with sample calculations for copper plating of multilayer boards.

## II. PROBLEM FORMULATION

A schematic cross section of a typical copper-plating tank is shown in Fig. 1. Copper anodes both provide current flow and replenish the plated metal in the solution. Cathodes, the multilayer boards, receive the plated metal and provide the return path for the current. The electroplating solution contains water, a salt of the plating metal, in this case $CuSO_4$, an acid to increase the conductivity of the solution, in this case $H_2SO_4$, and proprietary secret ingredients which improve the microscopic structure of the plated metal. The solution is well-stirred, and a flow of fresh solution past the cathodes is provided. In the typical tank, there are three different stirring mechanisms. First, the cathodes may be rocked back and forth along their width (perpendicular to the plane of Fig. 1) to reduce nonuniformity of plating from the bar anodes. Second, solution is pumped out of the tank near the bottom, filtered to remove foreign matter and granular copper, and then returned to the tank. Finally, each cathode has a sparger, or air bubbling pipe, under it, directing a stream of air bubbles up each side of the cathode and producing the convection pattern sketched in Fig. 1.

Other complications are, of course, possible and may be analyzed by the same program. Anodes and cathodes may be of more complex shapes; other metals or insulators may also be present, to alter the fluid flow or the distribution of plated metal on the cathode.

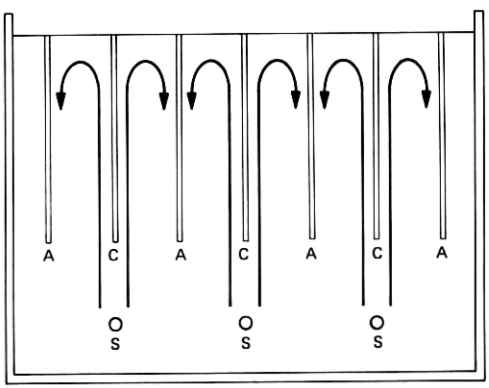


Fig. 1—Schematic cross section of a multilayer board plating tank, showing anodes (A), cathodes (C), and spargers (S).

Near the cathodes, bubbles from the spargers rise, causing a convection cell between each cathode-anode pair. For analyzing many of the possible effects, such as geometry, it is sufficient to assume a periodic tank, and to analyze only one convection cell, as in Fig. 2. (The program can analyze two-dimensional cells with arbitrary polygonal shapes, as well as three-dimensional axisymmetric cells with arbitrary polygonal cross section.) Very thin boundary layers, not shown in the figure, are adjacent to the electrodes. In the boundary layers, the copper concentration obeys a diffusion-convection equation. For velocity flows of the boundary layer type,

$$V_X = 2\,YE(X) \tag{1}$$

$$V_Y = -Y^2 \frac{dE(X)}{dX}, \tag{2}$$

the diffusion-convection equation in the boundary layer can be integrated approximately,[2] giving the concentration in terms of the current flow at the electrode.

The velocity fields in the boundary layers are needed. The velocity flow caused by bubbles rising near a vertical flat plate is complicated, and the solution for the flow is not known. However, the flow is qualitatively similar to the case of uniform flow past a flat plate, whose solution is available (Ref. 3, p. 125). If the flow far from the plate is $V_\infty$ in the $Y$ direction, the velocity field is as above, with

$$E(X) \approx 0.166[V_\infty^3/(\nu X)]^{1/2}. \tag{3}$$

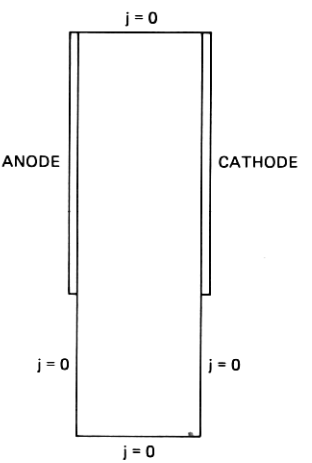


Fig. 2—One electroplating "cell." The parts of the boundary with no current flow are marked by $j = 0$.

With $s$ measuring distance along the cathode, the methods of Appendix II of Ref. 3 give

$$c(s) = 1 - \frac{1}{k_c} \int_0^s \frac{j(t)\, dt}{(s^{3/4} - t^{3/4})^{2/3}} \tag{4}$$

with the dimensionless parameter $k_c$ given by

$$k_c = \left[ \frac{32D^2}{3} \frac{0.166 V_\infty^{3/2}}{\nu^{1/2}} \right]^{1/3} \frac{\Gamma(\frac{2}{3})\, C_b F^2 X_0^{1/2}}{\kappa R_g T}. \tag{5}$$

The velocity field at the anodes is more difficult, since each anode is enclosed in a porous bag. The flow must be some kind of free convection, caused by the variation of electrolyte density with copper concentration. Since the only item of interest is the copper deposition distribution on the cathode, it seems unnecessary to include all the complications at the anode. Rather than assume a velocity field, a simple model for the concentration has been adopted. If $s$ measures distance along the anode, from the bottom,

$$c(s) = 1 + \frac{j(s)}{k_a s^\delta}. \tag{6}$$

This approximation is equivalent to assuming that the anode boundary layer has width proportional to $s^\delta$ and that the concentration varies linearly across the boundary layer. The effect on the cathode current distribution of various choices of $k_a$ and $\delta$ can be investigated later. Reasonable values of $\delta$ probably are in the range of from ¼ (free convection) to ½ (uniform flow past a flat plate).

The derivation of the equations describing copper plating is by now standard[1,2] and will not be repeated. The dimensionless variables we will need are the potential, $\phi$, the concentration of copper, $c$, and the current density flowing into the cathode, $j$. In our normalization, $j$ is equal to the directional derivative,

$$j = \frac{\partial \phi}{\partial \mathbf{n}}, \tag{7}$$

where $\mathbf{n}$ is the outward-pointing unit normal vector at each point of the cathode. The normalizations used are $X_0$ for lengths, $R_gT/F$ for potentials, $\kappa R_gT/X_0F$ for currents, and $C_b$, the bulk concentration, for the copper concentration.

Throughout the region shown in Fig. 2, outside the boundary layer, Laplace's equation holds:

$$\nabla^2 \phi = 0. \tag{8}$$

On the anode, the potential is a given constant, $\phi = \phi_a$. The cathode

is grounded. On the remaining boundaries, no current flows, $\partial\phi/\partial n = 0$. All the complication is in the nonlinear boundary conditions on the electrodes, coupling $\phi$ and $j$, in effect defining a nonlinear resistance of each boundary layer. The potential across the cathode boundary layer has two constituents,

$$\phi = \eta_s + \eta_c. \tag{9}$$

For the copper electroplating problem of interest, the concentration overpotential is

$$\eta_c = \tfrac{1}{2} \ln(c). \tag{10}$$

The surface overpotential is given by the relation

$$j = k_e c^{\gamma}(e^{\alpha_a \eta_s} - e^{-\alpha_c \eta_s}), \tag{11}$$

with the dimensionless parameter $k_e$ given by

$$k_e = \frac{FX_0 I_0}{\kappa R_g T}. \tag{12}$$

The boundary layer at the anode is treated similarly, although in practice the details are not important.

The problem is thus reduced to solving Laplace's equation in a rectangular region. There are linear boundary conditions on part of the boundary and complicated nonlinear boundary conditions on the remainder. An efficient technique for solving this problem is outlined in the next sections.

## III. SOLUTION OF LAPLACE'S EQUATION WITH NONLINEAR BOUNDARY CONDITIONS

We wish to solve Laplace's equation on a two-dimensional region, with boundary $B$. Let $s$ denote arc length on $B$. On the electrodes, a nonlinear boundary condition couples $\phi(s)$ and $j(s) = \partial\phi/\partial n$. On the rest of the boundary, $j(s) = 0$.

We first discuss solving Laplace's equation with nonlinear boundary conditions, assuming solutions with linear boundary conditions are available. In the next section, Laplace's equation with linear boundary conditions is discussed.

We expand the potential in terms of known solutions,

$$\phi = \sum_{l=1}^{L} d_l \phi_l, \tag{13}$$

and determine the $L$ coefficients $d_l$ so that the nonlinear boundary conditions are satisfied. Letting $j_l = \partial\phi_l/\partial n$, $\phi_l$ is defined to be a solution of Laplace's equation with $\phi_l = b_l(s)$ on the electrodes, and

$j_l(s) = 0$ on the rest of the boundary. The functions $b_l(s)$ are in principle arbitrary; $B$-splines are used as discussed in the next section.

Also choose $M$ points $s_m$ on the electrodes. $M \geq L$ is required; we use $M = 2L$. Suppose approximate values for the $d_l$'s are known. Then $j(s) = \sum_{l=1}^{L} d_l j_l(s)$ is the approximate current. From the integral formula, calculate the concentration $c(s_m)$ at $M$ points; then calculate the concentration overpotential $\eta_c(s_m)$. Then obtain the surface overpotential $\eta_s(s_m)$ by a Newton iteration. Finally, at $M$ points do a least-squares fit to

$$\eta_c(s) + \eta_s(s) = \sum_{l=1}^{L} d_l' b_l(s). \tag{14}$$

The differences, $d_l - d_l'$, are zero when the correct boundary conditions are obeyed.

The preceding paragraph defines a set of $L$ nonlinear equations for the $d_l'$'s. An initial guess is made, and the equations solved by a quasi-Newton iteration with rank-one update.[4,5] Usually only a few iterations, typically 5 to 10, are needed. Convergence is somewhat slower when the current is large, since the equations then are effectively more nonlinear.

In practice, the nonlinear equations are considerably less sensitive to the values of the $d_l'$'s on the anode than to those on the cathode, especially for high currents. This leads to difficulties in solving, since the Jacobian matrix is therefore ill-conditioned. This has been overcome by a two-step iteration process. First, $\phi$ on the anode is held fixed, and Laplace's equation is solved with nonlinear boundary conditions on the cathode. Second, the resulting $\phi$ on the cathode is held fixed, and Laplace's equation is solved with nonlinear boundary conditions on the anode. These two steps are repeated. Only two or three of these two-step iterations are needed.

## IV. LAPLACE'S EQUATION WITH LINEAR BOUNDARY CONDITIONS

To be able to deal with a wide variety of geometries, a boundary integral method is used. A more detailed discussion appears in Ref. 6.

We wish to solve $\nabla^2\phi = 0$ in a two-dimensional region with boundary $B$. On part of $B$, $B_1$, the boundary condition is $\phi = u(s)$; on the remainder, $B_2$, $j = \partial\phi/\partial n = 0$.

We start with Green's third boundary identity[7]

$$2\pi\phi(x, y) = \int_B \left[ \phi(s) \frac{\partial G}{\partial n} - j(s) G \right] ds. \tag{15}$$

Here $(x, y)$ is some point inside $B$, and $G$ is the "fundamental solution" to Laplace's equation,

$$G = -\tfrac{1}{2} \ln[(x_s - x)^2 + (y_s - y)^2]. \tag{16}$$

Also, $(x_s, y_s)$ are the coordinates of the point at arc length $s$ on $B$, and $\mathbf{n}(s)$ is the outward normal at $s$. In three dimensions with axial symmetry, the formulation is identical except for a different fundamental solution.

If $\phi(s)$ and $j(s)$ are replaced by other functions $\phi^*(s)$ and $j^*(s)$, the function $\phi$ defined by

$$2\pi\phi(x, y) = \int_B \left[ \phi^*(s) \frac{\partial G}{\partial n} - j^*(s) G \right] ds \tag{17}$$

exactly obeys Laplace's equation inside $B$, but does not obey the correct boundary conditions. The linear mixed boundary problem may be solved approximately by choosing functions $\phi^*(s)$ and $j^*(s)$ which make $\phi$ approximately obey the boundary conditions.

To do this, we parameterize $\phi^*$ and $j^*$ and determine reasonable values for the parameters. On $B_1$ we take

$$\phi^*(s) = u(s) \quad \text{and} \quad j^*(s) = \sum_{k=1}^{N_1} a_k b_k(s). \tag{18}$$

On $B_2$ we take

$$\phi^*(s) = \sum_{k=N_1+1}^{N_1+N_2} a_k b_k(s) \quad \text{and} \quad j^*(s) = 0. \tag{19}$$

The $a$'s are coefficients to be determined so that the boundary conditions are satisfied as closely as possible. The $b_k$ may be any useful set of functions. We use $B$-splines.[8,9] As a basis function for $j^*$, a function behaving like the inverse square root of distance from the lower end of each electrode may be used, in addition. Such a term is present in the primary current, though not in the solution to the nonlinear problem. Inclusion of this basis function affects the result only very near the end of the electrode; its inclusion assures that far fewer basis functions are necessary for good accuracy. This basis function is included in the sample calculations; its use in the program is optional.

If $(x, y)$ approaches, from inside $B$, a point at arc length $t$ at a smooth part of $B$, it may be shown[7] that the $2\pi$ in (17) changes to a $\pi$ and the line integral becomes a Cauchy principal value integral. Then we have

$$\begin{aligned} &t \text{ on } B_1: \pi u(t) \\ &t \text{ on } B_2: \pi \sum_{k=N_1+1}^{N_1+N_2} a_k b_k(t) \end{aligned} = \int_{B_2} \sum_{k=1}^{N_1} a_k b_k(s) \frac{\partial G}{\partial n} \, ds + \int_{B_1} \left[ u(s) \frac{\partial G}{\partial n} - G \sum_{k=N_1+1}^{N_1+N_2} a_k b_k(s) \right] ds, \tag{20}$$

where the integrals are to be interpreted as Cauchy principal value

integrals at $s = t$. For any particular point $t_j$, this equation reduces to the form

$$r_j = \sum_{k=1}^{N_1+N_2} A_{jk} a_k, \tag{21}$$

where $A_{jk}$ involves integrals of $b_k(s)$, and $r_j$ an integral of $u(s)$. Some of the integrals are singular, and require some care.[6] Equation (20) cannot be made to hold for all $t$ on $B$, since there are only $N_1 + N_2$ $a$'s. An approximate solution for the $a$'s can be found by choosing $N_3$ points $t_j$, $N_3 > N_1 + N_2$, and doing a least-squares fit of the $N_3$ linear equations in $N_1 + N_2$ unknowns.

The resulting $a_k$'s give $\phi^*(s)$ and $j^*(s)$ directly, with no need to perform any derivatives. An error estimate for $\phi$ may be obtained by comparing $\phi^*(t)$ and the $\phi(t)$ obtained from the integral definition, letting $t \to B$.

In practice, a second integral equation is also used, to improve the conditioning of the $A_{jk}$ matrix. Details are in Ref. 6.

## V. SAMPLE CALCULATIONS

In this section, sample calculations are presented for a typical tank. Its dimensions are cathode length 46 cm, anode length 46 cm, cathode-anode separation 16 cm, and total tank depth 84 cm. We use $X_0 = 46$ cm. The three major components of the electrolyte are $Cu^{++}$, $H^+$, and $HSO_4^-$. The bulk concentrations are approximately 0.27 molar $CuSO_4$ and 1.7 molar $H_2SO_4$. The bulk solution has a concentration of copper ions of $C_b = 0.00027$ moles/cm$^3$. The bulk conductivity, $\kappa$, is obtained using data in Newman[1] for mobilities, giving $\kappa = 0.63(\text{ohm—cm})^{-1}$. Also $D = 0.55 \times 10^{-5}$ cm$^2$/s and $\nu = 0.01 \times 10^{-5}$ cm$^2$/s. Then the dimensionless parameters are $\alpha$, $\beta$, $\gamma$, $\delta$, $k_a$, $k_c$, and $k_e$. The remaining material constants are taken to be:[10] $\alpha_c = 1.5$, $\alpha_a = 0.5$, and $\gamma = 0.42$. Also from Ref. 10, $I_0 = 0.001$ amp/cm$^2$. We obtain $k_c \approx 26\, V_\infty^{1/2}$ and $k_c \approx 2.5$.

Using $k_c = 260$ and $\phi_a = 30$, the first set of sample calculations tested the dependence of $j(x)$ and $c(x)$ on the anode parameters $k_a$ and $\delta$. With $k_a = 50$, values of $\delta$ used were $-\frac{1}{2}$, $-\frac{1}{4}$, 0, and $+\frac{1}{2}$; with $\delta = -\frac{1}{4}$, values of $k_a$ used were 10, 50, and 250. As hoped and expected, $j(x)$ and $c(x)$ at the cathode were quite insensitive to the choices of the anode parameters $k_a$ and $\delta$, varying by only a few percent over all the choices of anode parameters. For the remainder of the sample calculations, $k_a = 50$ and $\delta = -\frac{1}{4}$.

The second set of calculations varied the applied potential, $\phi_a$, keeping $k_c = 260$. Figures 3 and 4 show $j(x)$ and $c(x)$, for $\phi_a = 20$, 30, and 40, as well as their limiting distributions and the primary current distribution. (In Figure 3, the curve for $\phi_a = 30$ has been omitted; it is

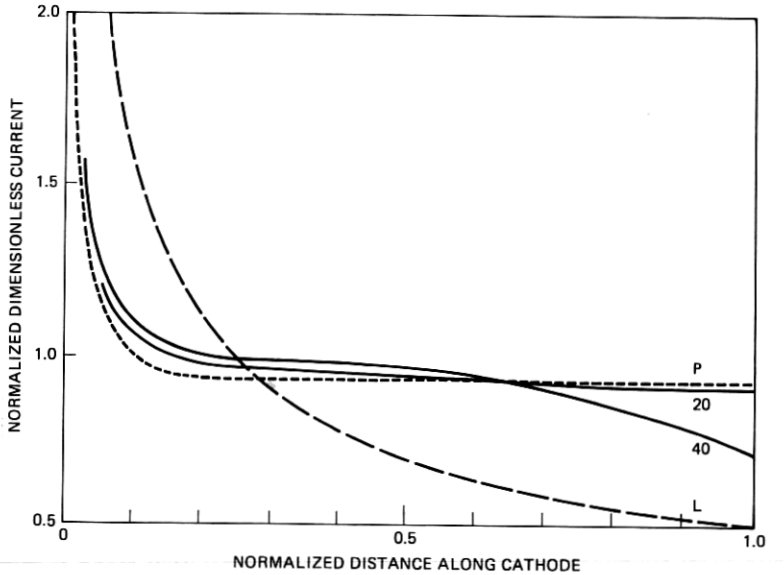


Fig. 3—Normalized plating thickness distribution on cathode for anode potentials $\phi_a = 20$ and 40. Other parameters are $k_a = 50$, $\delta = -1/4$, and $k_c = 260$. For comparison, the primary distribution (P) and the limiting distribution (L) are also shown.

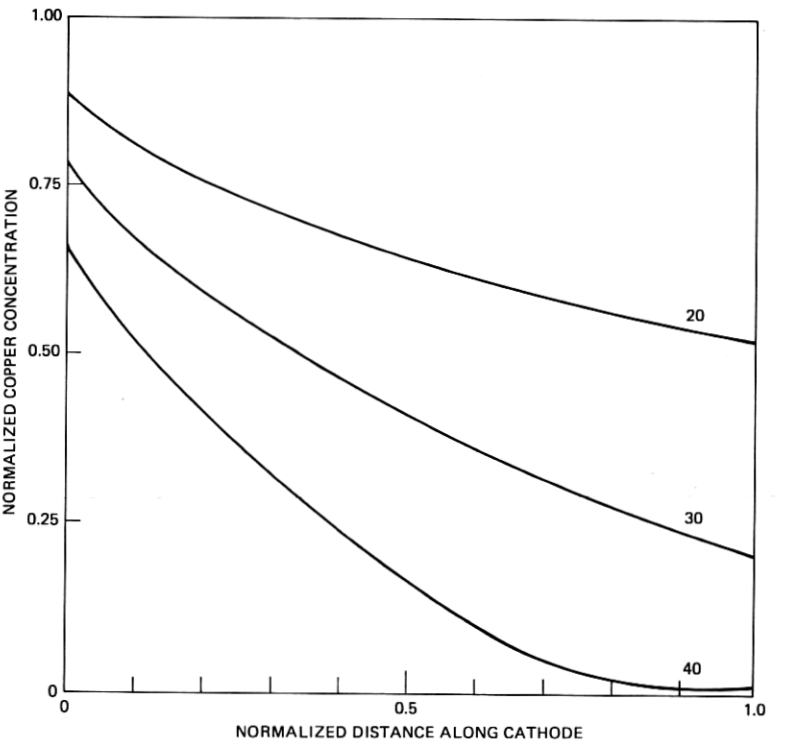


Fig. 4—Copper concentration on cathode for anode potentials $\phi_a = 20$, 30, and 40. Other parameters are $k_a = 50$, $\delta = -1/4$, and $k_c = 260$.

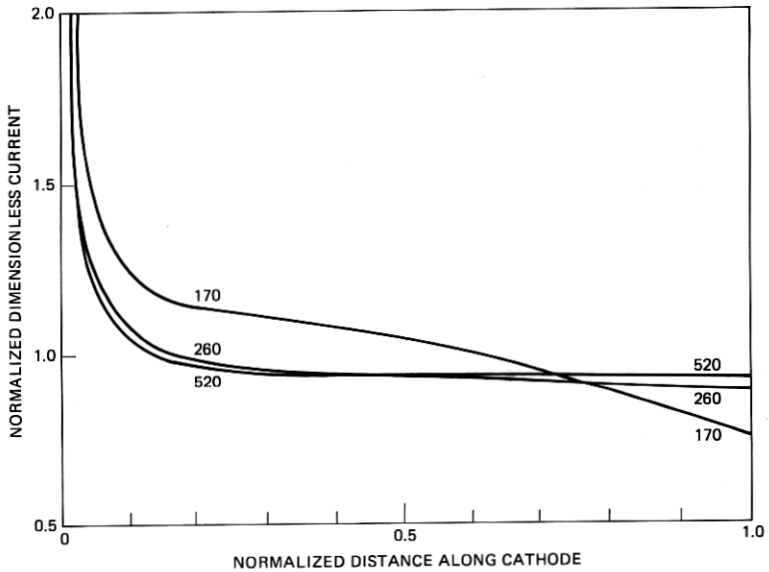


Fig. 5—Normalized plating thickness distribution on cathode for $k_c$ = 170, 260, and 520. Other parameters are $\phi_a$ = 30, $k_a$ = 50, and $\delta = -1/4$.

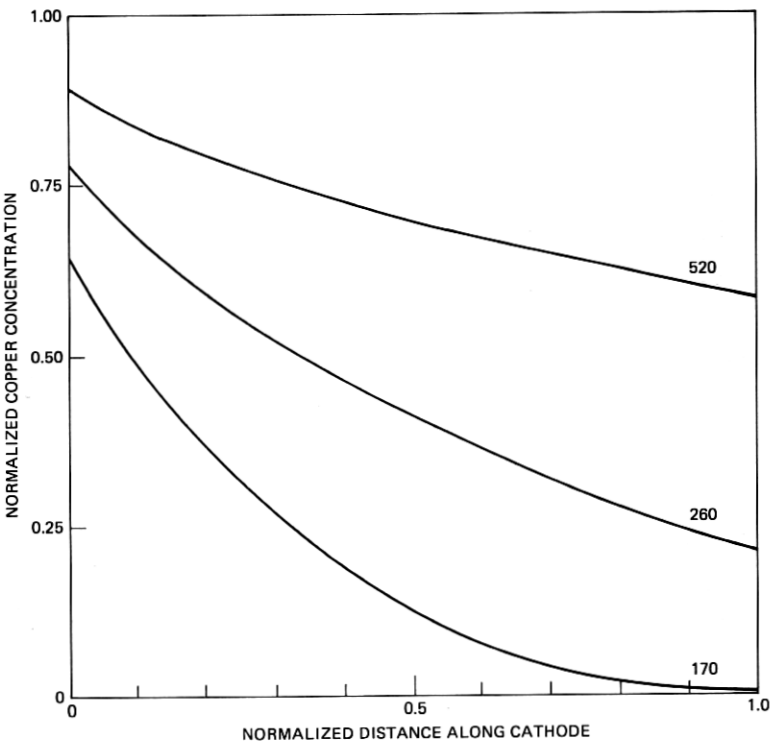


Fig. 6—Copper concentration on cathode for $k_c$ = 170, 260, and 520. Other parameters are $\phi_a$ = 30, $k_a$ = 50, and $\delta = -1/4$.

almost identical to that for $\phi_a = 20$.) Each $j(x)$ curve has been normalized to its mean value, to emphasize the shapes of the curves. The primary current distribution is the current derived from solving Laplace's equation with linear boundary conditions, assuming zero potential drop across the concentration boundary layers. Recall that $j(x)$ is proportional to the rate of deposition of copper on the cathode, and therefore is proportional to the plating thickness distribution. As the applied potential increases, the concentration of copper in solution at the cathode decreases. This decrease does not significantly change the shape of the $j(x)$ curve from $\phi_a = 20$ to $\phi_a = 30$. At $\phi_a = 40$, $c(x)$ becomes quite small near $x = 1$; the potential between the bulk and the cathode, $\eta_c(x) + \eta_s(x)$, becomes large; and the $j(x)$ curve changes shape. With still higher applied potential, $j(x)$ becomes less uniform. A limiting current is defined as the $j(x)$ in (4), which makes $c(x)$ identically zero,

$$i_{\text{lim}}(x) = \frac{3k_c}{4\Gamma(\frac{2}{3})\Gamma(\frac{1}{3})x^{1/2}} \approx 0.207\,\frac{k_c}{x^{1/2}}. \tag{22}$$

Since $\eta_c(x)$ is proportional to $\ln c(x)$, the limiting current requires infinite applied potential. For Fig. 3, the total currents are approximately 35, 58, and 79 percent of the total limiting current, for $\phi_a = 20$, 30, and 40, respectively. Practical copperplating usually is done at a

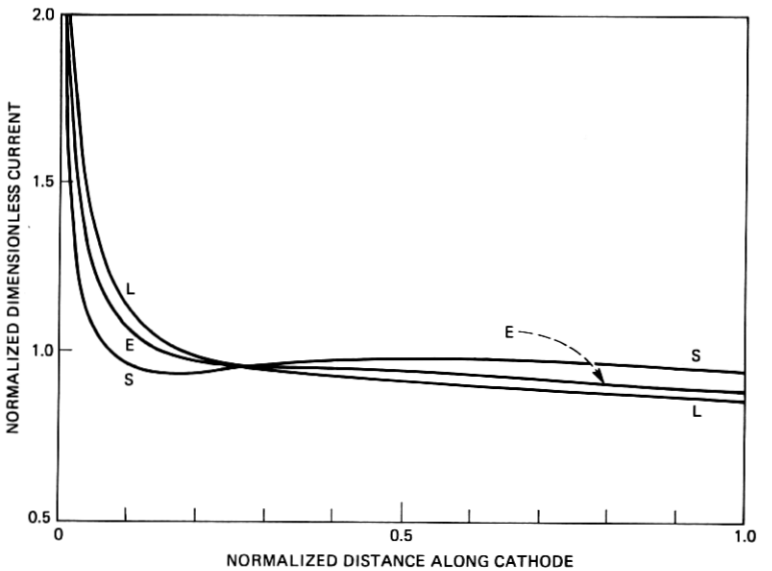


Fig. 7—Normalized plating thickness distribution on cathode for anode lengths of 41 cm (S), 46 cm (E), and 51 cm (L). Other parameters are $\phi_a = 30$, $k_a = 50$, $\delta = -\frac{1}{4}$, and $k_c = 260$.

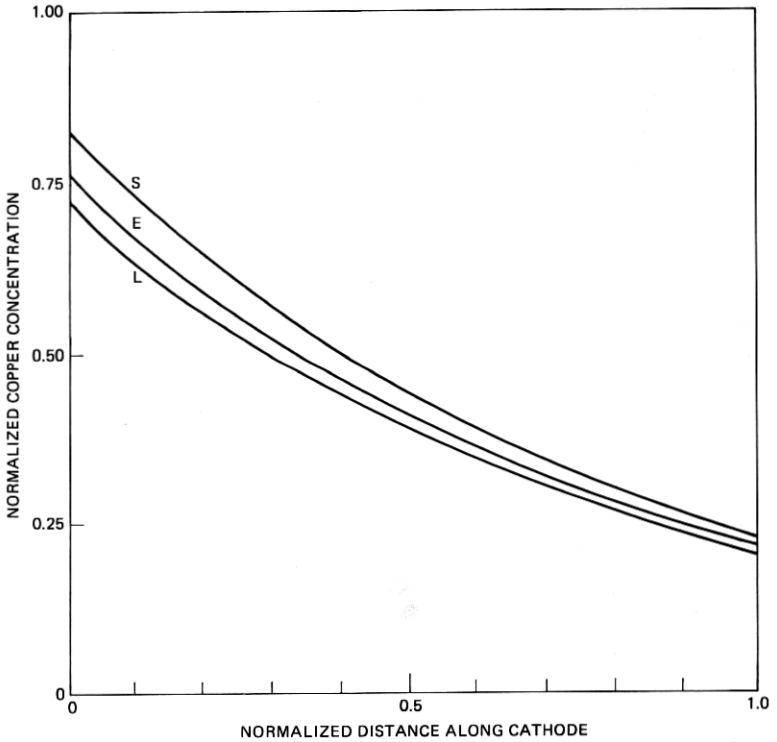


Fig. 8—Copper concentration on cathode for anode lengths of 41 cm (S), 46 cm (E), and 51 cm (L). Other parameters are $\phi_a = 30$, $k_a = 50$, $\delta = -1/4$, and $k_c = 260$.

total current less than one-quarter of the total limiting current. These elaborate calculations demonstrate that, for these typical copperplating conditions, the primary current distribution is quite adequate for predicting the plating thickness distribution. In the remaining calculations, $\phi_a = 30$ is used.

The third set of calculations varies the cathode parameter $k_c$, which is proportional to the square root of the fluid velocity. Figures 5 and 6 show the results. If $k_c$ is too small, the current becomes quite nonuniform. For the remaining calculations, $k_c = 260$.

The final set of calculations shows the effect of anode length. Anode lengths of 41, 46, and 51 cm were used; the cathode length was left at 46 cm. Figures 7 and 8 show the results. With the shorter anode, the current was within ±10 percent over more of the cathode than with a longer anode.

## APPENDIX

### Symbols

| | |
|---|---|
| $a_k$ | Unknown coefficient in solution of Laplace's equation. |
| $A_{jk}$ | Matrix element. |
| $b_l$ | Function in expansion of boundary values. |
| $B$ | Boundary of region. |
| $B_1$ | Part of boundary on which $\phi$ is given. |
| $B_2$ | Part of boundary on which no current flows. |
| $c$ | Normalized copper concentration, dimensionless. |
| $C_b$ | Bulk copper concentration, g-mole/cm$^3$. |
| $d_l, d'_l$ | Coefficients in expansion of overpotential. |
| $D$ | Diffusion coefficient, cm$^2$/s. |
| $E$ | Velocity field function, s$^{-1}$. |
| $F$ | Faraday's constant, 96500 coul/g-equivalent. |
| $G$ | Fundamental solution to Laplace's equation. |
| $I_0$ | Exchange current density, A/cm$^2$. |
| $j, j^*$ | Normalized current density, dimensionless. |
| $j_l$ | Normalized current density of $l$th solution, dimensionless. |
| $j_{\text{lim}}$ | Limiting current distribution, dimensionless. |
| $k_a, k_c, k_e$ | Dimensionless constants. |
| $L$ | Number of coefficients in expansion of overpotential. |
| $M$ | Number of fitting points for overpotential expansion. |
| $N_1$ | Number of coefficients in expansion of $j$ on $B_1$. |
| $N_2$ | Number of coefficients in expansion of $\phi$ on $B_2$. |
| $N_3$ | Number of fitting points in solution of Laplace's equation. |
| $n$ | Directional derivative, in $\partial\phi/\partial n$ and $\partial G/\partial n$. |
| $\mathbf{n}$ | Unit vector in outward normal direction. |
| $r_j$ | Matrix element. |
| $R_g$ | Universal gas constant, 8.21 joules/g-mole deg. |
| $s, t$ | Arc length along boundary, dimensionless. |
| $s_m$ | Fitting points on boundary. |
| $T$ | Absolute temperature, degrees Kelvin. |
| $u$ | Boundary condition for $\phi$. |
| $V_X, V_Y$ | Components of fluid velocity, cm/s. |
| $V_\infty$ | Fluid velocity far from plate, cm/s. |
| $x, y$ | Coordinates, dimensionless. |
| $x_s, y_s$ | Coordinates of point at distance $s$ along electrode. |
| $X, Y$ | Coordinates, cm. |
| $X_0$ | Normalizing length, cm. |
| $\alpha_a, \alpha_c, \gamma$ | Parameters in reaction rate expression, dimensionless. |
| $\delta$ | Exponent in concentration at anode, dimensionless. |

$\Gamma$ Gamma function.

$\eta_c$ Concentration overpotential, dimensionless.

$\eta_s$ Surface overpotential, dimensionless.

$\kappa$ Bulk electrolyte conductivity, $(\text{ohm—cm})^{-1}$.

$\nu$ Viscosity, $\text{cm}^2/\text{s}$.

$\phi$, $\phi^*$ Normalized potential, dimensionless.

$\phi_a$ Anode voltage, dimensionless.

$\phi_l$ Potential for $l$th solution of Laplace's equation, dimensionless.

## REFERENCES


1. J. R. Newman, *Electrochemical Systems*, Englewood Cliffs, N.J.: Prentice-Hall, 1973.
2. W. H. Smyrl and J. R. Newman, J. Electrochem. Soc., *119* (1972), pp. 212–219.
3. H. Schlichting, *Boundary-Layer Theory*, New York: McGraw-Hill, 1968.
4. C. G. Broyden, Math. Comp., *19* (1965), pp. 577–593.
5. J. L. Blue, "Robust Methods for Solving Systems of Nonlinear Equations," SIAM J. on Scientific and Statistical Computing, to be published (1980).
6. J. L. Blue, "Boundary Integral Solutions of Laplace's Equation," B.S.T.J. *57*, No. 8 (October 1978), pp. 2797–2822.
7. O. D. Kellogg, *Foundations of Potential Theory*, New York: Dover, 1953 (reprint of original 1929 edition).
8. H. B. Curry and I. J. Schoenberg, J. Anal. Math., *17* (1966), pp. 71–107.
9. C. de Boor, J. Approx. Th., *6* (1972), pp. 50–62.
10. V. Marathe and J. R. Newman, J. Electrochemical Soc., *116* (1969), pp. 1704–1707.